Plate-mode waves in phononic crystal thin slabs: Mode conversion

Jiu-Jiu Chen and Bernard Bonello*

Institut des NanoSciences de Paris, CNRS (UMR 7588), Université Pierre et Marie Curie, 140 rue de Lourmel, 75015 Paris, France

Zhi-Lin Hou

Laboratoire de Physique des Milieux Ionisés et Applications (LPMIA), Nancy University-CNRS, Boulevard des Aiguillettes, BP 239, 54506 Vandoeuvre-lès-Nancy, France

(Received 18 February 2008; revised manuscript received 23 June 2008; published 25 September 2008)

We have computed the dispersion curves of plate-mode waves propagating in periodic composite structures composed of isotropic aluminum cylinders embedded in an isotropic nickel background. The phononic crystal has a square symmetry and the calculation is based on the plane-wave expansion method. Along ΓX or ΓM directions, shear-horizontal modes do not couple to the Lamb wave modes which are polarized in the sagittal plane. Whatever the direction of propagation in between ΓX and ΓM, shear-horizontal modes convert to Lamb waves and couple with the flexural and dilatational modes. This phenomenon is demonstrated both through the mode splitting in the lower-order symmetric band structure and through the calculation of all three components of the particle displacements. The phononic case is different from the pure isotropic plate case where shear-horizontal waves decouple from Lamb waves whatever the direction of propagation.

DOI: 10.1103/PhysRevE.78.036609 PACS number(s): 43.20.+g, 63.20.−e, 43.40.+s, 41.20.Jb

In the last past decade, the existence of forbidden gaps in the band structure of acoustic and elastic waves propagating in periodic composite materials has received a great deal of attention. For frequencies within the band gap, the propagation of acoustic or elastic waves is forbidden regardless of the direction, suggesting numerous technological applications such as acoustic filters, ultrasonic silent blocks, acoustic mirrors, etc. Such composite structures for bulk, surface, or plate-mode waves have been studied both theoretically [1–11] and, in a less extent, experimentally [12–14] by many groups. In particular, there has been a growing interest for Lamb waves and plate modes which can be used for a variety of high-frequency applications such as physical, chemical, and biological sensors.

Strictly speaking, a plate can support an infinite number of guided waves with nonzero cutoff frequencies, which all are solutions of the dispersion relation. However, in practice, a thin plate admits a number of antisymmetric and symmetric Lamb waves and shear-horizontal (SH) waves, which depends on the value of the ratio h/λ, where h and λ are, respectively, the thickness of the plate and the acoustic wavelength. Recently, Chen *et al.* [15] used a plane-wave expansion method (PWE) to calculate the band structures of lowest-order Lamb waves propagating perpendicularly to the alternating layers of one-dimensional (1D) phononic crystal thin plates. They have shown that, in these 1D phononic slabs, SH waves decouple from the Lamb waves and that the ratio of the plate thickness to the lattice spacing is the most important parameter for the formation of band gaps in Lamb modes, but not in SH mode. A similar result was found recently in the two-dimensional (2D) case by Sun *et al.* [16] who studied the propagation of Lamb waves along ΓX in 2D phononic crystal plates with a square lattice. In homogeneous plates, SH waves only exist if the material is isotropic. In that case, three types of the free plate modes must be considered, namely the pure shear-horizontal mode which polarization is parallel to the free surfaces; this SH mode is uncoupled from the two others modes: The dilatational and the flexural modes. This greatly simplifies the investigation of Lamb wave motion in the isotropic materials. When the material is anisotropic, SH modes are still solutions for the equations of motion, but only along some particular directions of high symmetry. Outside these particular solutions, there is no longer a family of pure shear-horizontal modes independent from the dilatational and flexural modes: All partial waves are coupled and the free plate modes can only be classified either as symmetric or as antisymmetric modes with respect to the median plane.

However, in a phononic crystal made of two isotropic materials, SH waves cannot exist in the same way as in the pure isotropic plates. Indeed, Sun *et al.* [16] have demonstrated by using a finite-difference time-domain technique, that when waves propagate along the ΓX direction in the 2D phononic crystals, thin plates consisting of an array of isotropic steel cylinders embedded in an isotropic epoxy matrix, SH waves decouple from Lamb waves. To our knowledge, this property has not been studied for propagation along other directions of the irreducible Brillouin zone so far.

In this paper, we analyze the relationship between SH waves and Lamb waves in 2D phononic crystal plates consisting of a square array of isotropic aluminum (Al—material A) cylinders embedded in an isotropic nickel (Ni—material B) background, for propagation along any direction of the irreducible Brillouin zone. To this end, one must solve the equations of motion

$$\rho(\mathbf{x})\frac{\partial u_i}{\partial t^2}=\frac{\partial}{\partial x_j}\left(C_{ijkl}(\mathbf{x})\frac{\partial u_l}{\partial x_k}\right), \tag{1}$$

where both the density $\rho(\mathbf{x})$ and the elastic stiffness tensor $C(\mathbf{x})$ are periodic functions of the in-plane components $\mathbf{x}=(\mathbf{x}_1,\mathbf{x}_2)$. Due to the artificial anisotropy of the medium, there are no analytical solutions to this equation and numeri-

*Corresponding author; bernard.bonello@insp.jussieu.fr

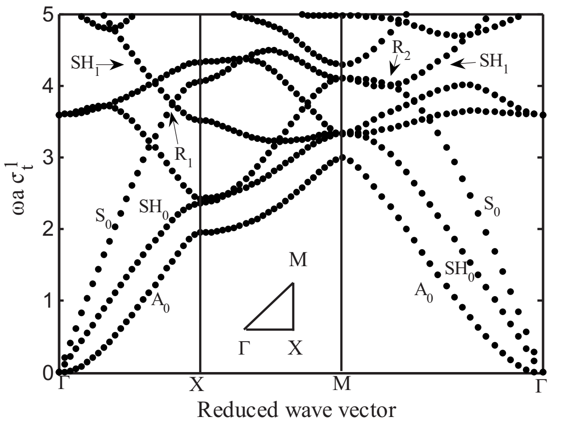

FIG. 1. Dispersion curves of plate waves in a phononic crystal with the square lattice symmetry. (Al cylinders in a Ni background; f=0.6, h/a=0.8).

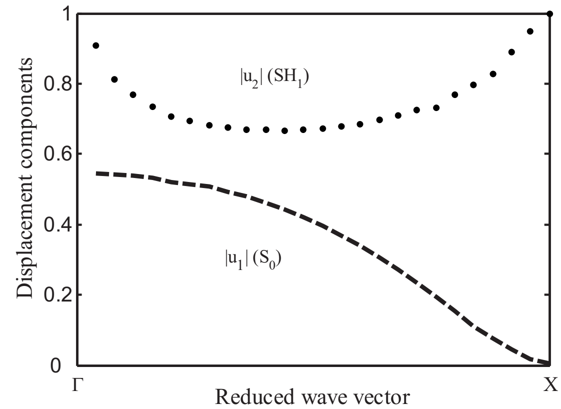

FIG. 2. Displacement components of SH_1 and S_0 along ΓX.

cal schemes are generally implemented to calculate the displacement vector $\mathbf{u}(\mathbf{x},\mathbf{x}_3,t)$ in the system. Different methods have been proposed, among which the PWE is one of the simplest. Basically, it consists in taking advantage of the periodicities along $\mathbf{x}_1$ and $\mathbf{x}_2$ to expand $\mathbf{u}$, C and ρ in Fourier series and in solving Eq. (1) in the reciprocal space. Boundary conditions are then introduced to account for the particular geometry of the system under study, leading generally to CPU-time-consuming computations. We rather used a supercell PWE method. A comprehensive description of this method is out of the scope of this paper and we give here only the main outlines [17]. In short, it consists in building a fictitious three-dimensional (3D) periodic system by staking along the out-of-plane direction $\mathbf{x}_3$ a unit cell consisting of the actual PC, surrounded by vacuum layers. The dispersion curves of the actual 2D PC are then deduced from the Fourier transform of the equations of motion in this fictitious medium. Since the vacuum layers avoid the coupling of the vibrational modes between adjacent PC layers, deriving the dispersion curves of the PC does not require writing explicitly the boundary conditions on the free surfaces [18–20].

The lowest-order dispersion curves for the plate waves propagating along the boundaries of the irreducible part of the Brillouin zone are shown in Fig. 1. In the calculation, we fixed the filling fraction to f=0.6 and the thickness-lattice spacing ratio was h/a=0.80. The physical parameters of aluminum and nickel used in the numerical calculations are given in Ref. [5]. The vertical axis in Fig. 1 is the normalized frequency $\omega^*=\omega a/C_t$, where C_t stands for $(\bar{C}_{44}/\bar{\rho})^{1/2}$; $\bar{C}_{44}=fC_{44}^A+(1-f)C_{44}^B$ and $\bar{\rho}=f\rho_A+(1-f)\rho_B$ are the effective elastic stiffness tensor and density, respectively. The horizontal axis is the reduced wave number $k^*=ka/\pi$. In the calculations, $\mathbf{x}_1$ and $\mathbf{x}_2$ axes were parallel to the edges of the square unit cell. To insure very good convergence of the computations, we considered 25 reciprocal vectors in the propagation plane $(\mathbf{x}_1,\mathbf{x}_2)$ and five Fourier components along the out-of-plane direction $\mathbf{x}_3$. Moreover, we have only considered the low-frequency part of the Brillouin zone ($\omega^*\leqslant 5$ in reduced units) where the lowest-order SH waves along ΓX and ΓM propagation directions are the fundamental first modes in the band structure.

When the plate waves propagate along ΓX, the SH wave and Lamb waves are decoupled and the fundamental symmetric Lamb wave (S_0) crosses over the SH_1 wave at a point denoted R_1 in Fig. 1. To further examine whether this intersection is real or apparent, we have calculated the displacement fields associated to SH_1 and S_0 modes while propagating along ΓX. The results are displayed in Fig. 2 where we show the magnitudes of the components u_1 for S_0 and u_2 for SH_1. Note that both S_0 and SH_1 have in-plane polarization for propagation along ΓX and that u_1 (respectively, u_2) is the only nonzero component for S_0 (respectively, SH_1). Whatever the wave-number value along ΓX, both components are different from zero and therefore, R_1 is actually a crossing point. It is also interesting to notice that the component u_1 for S_0 goes to zero at X point. For comparison, we have calculated its magnitude at X point, for the high-frequency edge of the gap ($\omega a/c_t$=5.3—not shown in Fig. 1). We found $|u_1|\approx 2$, about 2 times as large as the component $|u_2|$ of SH_1.

We have then calculated the lowest-order dispersion curves for plate waves with $\mathbf{k}$ vector making an angle φ =5°, 15°, 30°, and 40° with respect to the direction ΓX in the reduced Brillouin zone. The results are shown in Figs. 3(a)–3(d). As soon as φ departs from 0°, and because of the anisotropy of the effective velocity in this phononic crystal made of two isotropic materials, the sagittal plane (i.e., the plane parallel both to $\mathbf{k}$ and to $\mathbf{x}_3$) is no longer a plane of symmetry [21,22] and there is no longer a family of SH modes independent from the flexural and the dilatational modes. All partial waves are coupled and the free plate modes can only be classified as symmetric or antisymmetric with respect to the midplane of the plate [23]. In that case, as shown in Fig. 3, a splitting occurs at points T_1, T_2, T_3, and T_4, which are equivalent to the crossing point R_1 in Fig. 1 (φ=0°). A physical explanation for this splitting can be found from the conversion between SH waves and symmetric Lamb waves: When two plate waves intersect, those modes will split rather than cross if plate modes are of the same symmetry [23]. The sharp bends of the dispersion curves induce a band gap which is much larger for plate waves than it is for bulk waves [8]. Moreover, the magnitude of this band gap depends on the angle φ; we measured the values 0.1858, 0.5109, 0.6853, and 0.2588 around points T_1, T_2, T_3, and T_4 respectively. When the plate waves propagate

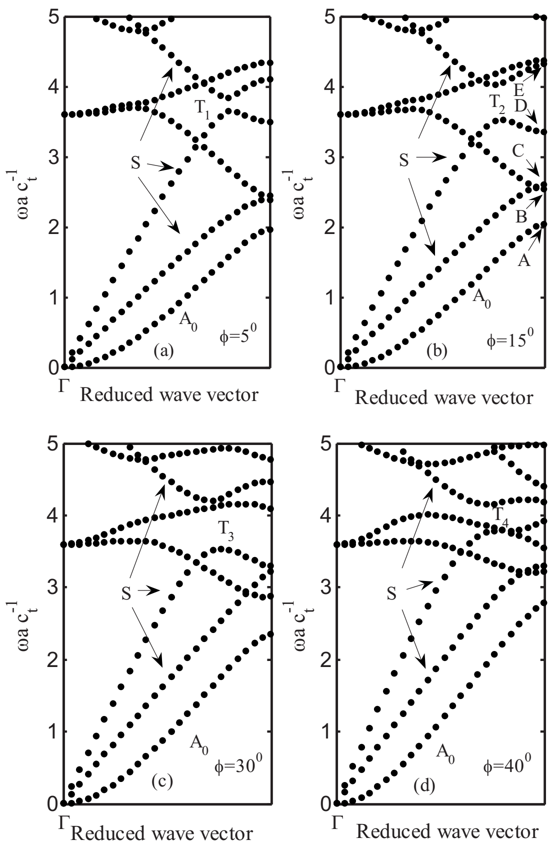

FIG. 3. Dispersion curves of plate waves for different angles: $\varphi=5°$ (a), $\varphi=15°$ (b), $\varphi=30°$ (c), $\varphi=40°$ (d).

along ΓM ($\varphi=45°$), the sagittal plane is again a plane of mirror symmetry, just as for propagation along ΓX ($\varphi=0°$). Therefore, the dispersion curves of the free plate vibrations can again be classified into the three families: Flexural, dilatational, and SH, as show in the right-hand panel in Fig. 1 where the shear-horizontal mode SH_1 intersects the fundamental dilatational mode S_0 at point R_2, similar to point R_1 in the left-hand panel.

In order to check to which extent our findings can be generalized, we have investigated the propagation at $\varphi=15°$, in a phononic plate with the same composition but with different values of both the filling fraction and the thickness to lattice parameter ratio. The results for ($f=0.2$, $h/a=0.80$) and ($f=0.6$, $h/a=0.20$) are displayed in Figs. 4(a) and 4(b), respectively. We have also studied how these results are modified when one considers inclusions made of a material harder than the background, as this is the case for Ni cylinders embedded in an Al plate. The result is displayed in Fig. 4(c). It is clear from Fig. 4 that the band gap in the splitting region is not strongly affected by either the geometrical parameters, or by the composition of the phononic plate.

To further understand the peculiar behavior of the plate modes at T_1, T_2, T_3, and T_4, we have computed, for $\varphi=15°$, the displacement fields in the thickness of the plate, below a selected point in the unit cell: The center of the Al cylinder. The symmetries being conserved between the points T and the edge of the reduced Brillouin zone, we have calculated

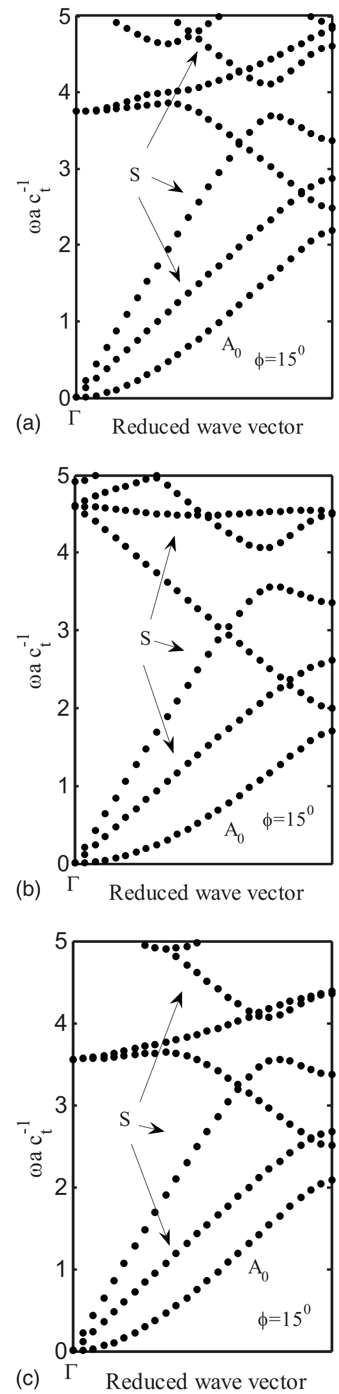

FIG. 4. Dispersion curves of plate waves for different parameters: $f=0.2$ and $h/a=0.80$ Al/Ni square lattice symmetry (a), $f=0.6$ and $h/a=0.2$ Al/Ni square lattice symmetry (b), $f=0.6$ and $h/a=0.80$ Ni/Al square lattice symmetry (c).

the displacement fields at points located along XM. Shown in Fig. 5 are the relative amplitudes of the displacement fields calculated at points A, B, C, D, and E in Fig. 3(b). The dotted, dashed, and full lines in Fig. 5, refer, respectively, to u_1, u_2 and u_3. It is clear from this figure that the displacements are either symmetric or antisymmetric with respect to the midplane of the plate. Indeed, at points A and B, both real and imaginary parts of u_3 have antisymmetric variations, whereas u_1 and u_2 exhibit symmetric behaviors. This is the

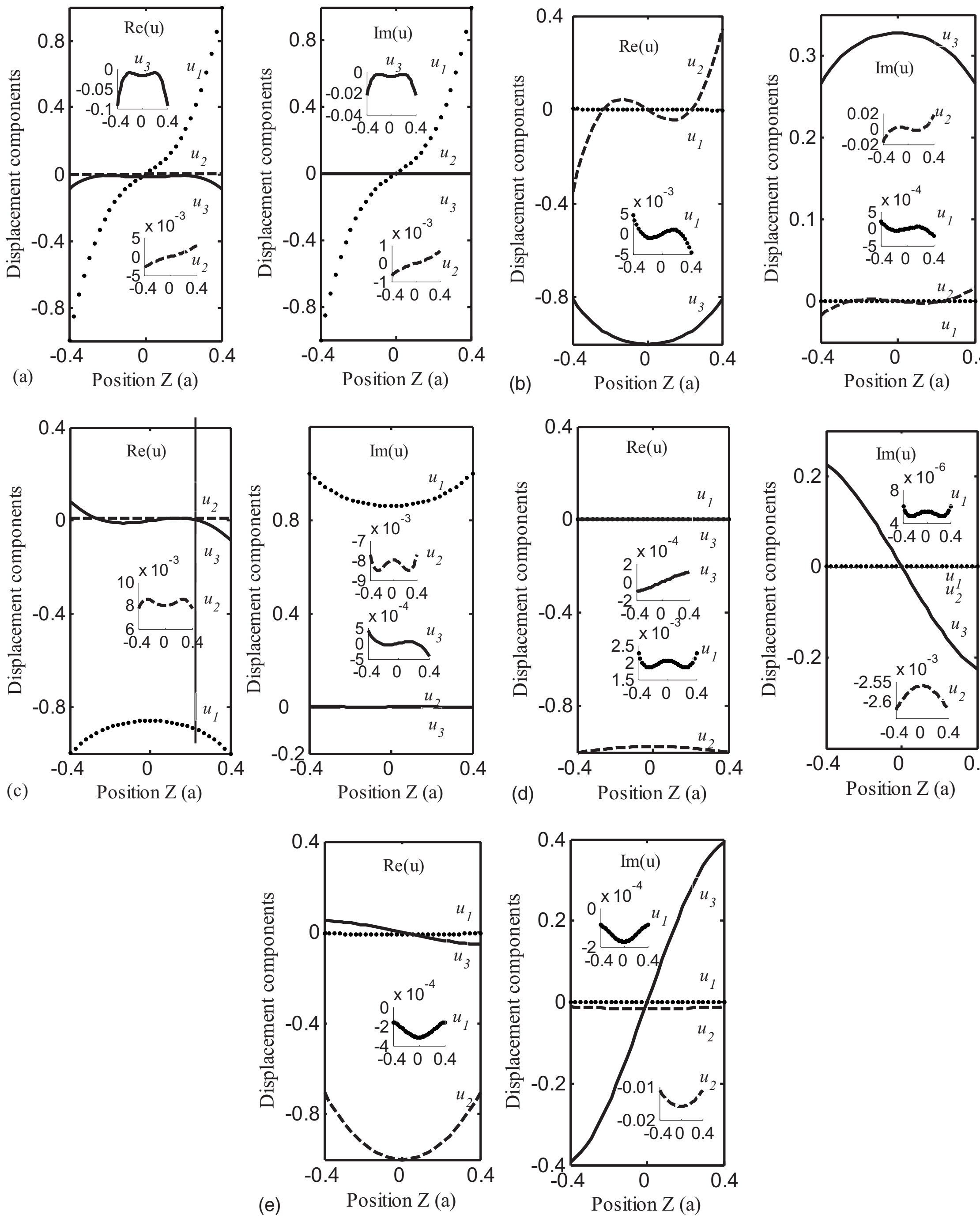

FIG. 5. Displacement components of plate waves propagating in a Al/Ni phononic crystal (f=0.6, h/a=0.8) calculated at points A, B, C, D, and E in Fig. 3(b), as a function of the distance from the midplane. The unit of the horizontal axis refers to the lattice parameter a; dotted, dashed, and solid lines correspond, respectively, to u_1, u_2, and u_3.

opposite situation at points C, D, and E where both real and imaginary parts of u_3 are symmetric, whereas the real and imaginary parts of u_1 and u_2 are antisymmetric with respect to the midplane of the plate. This analysis confirms that the vibrational modes at points A and B are antisymmetric Lamb waves, and symmetric Lamb waves [24] at points C, D, and E.

In conclusion, we have investigated the propagation of plate waves along all directions of the irreducible Brillouin zone of a phononic crystal thin slab. Along the ΓX or ΓM directions, SH modes do not couple to the Lamb waves polarized in the sagittal plane. Between ΓX propagation and ΓM propagation direction, SH modes convert to Lamb wave modes and couple with the flexural and dilatational modes, giving rise to a splitting of the mode.

J.-J. Chen is indebted to “La Ville de Paris” for financial support.

[1] M. S. Kushwaha, P. Halevi, L. Dobrzynski, and B. Djafari-Rouhani, Phys. Rev. Lett. **71**, 2022 (1993).
[2] M. S. Kushwaha, P. Halevi, and G. Martínez, L. Dobrzynski, and B. Djafari-Rouhani, Phys. Rev. B **49**, 2313 (1994).
[3] M. Wilm, A. Khelif, S. Ballandras, V. Laude, and B. Djafari-Rouhani, Phys. Rev. E **67**, 065602(R) (2003).
[4] Z. L. Hou, X. J. Fu, and Y. Y. Liu, Phys. Rev. B **73**, 024304 (2006).
[5] We used the elastic constants $C_A^{11}=11.1$, $C_A^{12}=6.1$, and $C_A^{44}=2.5$ (in units of 10^{11} dyn/cm^2) and mass density $\rho_A=2.695$ g/cm^3 for aluminum, and mass $C_B^{11}=32.4$, $C_B^{12}=16.4$, and $C_B^{44}=8$ (in units of 10^{11} dyn/cm^2) and mass density $\rho_B=8.905$ g/cm^3 for nickel from T. T. Wu, Z. G. Huang, and S. Lin, Phys. Rev. B **69**, 094301 (2004).
[6] M. Wilm, S. Ballandras, V. Laude, and T. Pastureaud, J. Acoust. Soc. Am. **112**, 943 (2002).
[7] J. J. Chen, B. Qi, and J. C. Cheng, Chin. Phys. Lett. **22**, 1706 (2005).
[8] C. Charles, B. Bonello, and F. Ganot, Ultrasonics **44**, e1209 (2006).
[9] T. T. Wu and Z. G Huang, Phys. Rev. B **70**, 214304 (2004).
[10] J. O. Vasseur, A.-C. Hladky-Hennion, B. Djafari-Rouhani, F. Duval, B. Dubus, Y. Pennec, and P. A. Deymier, J. Appl. Phys. **101**, 114904 (2007).
[11] A. Khelif, B. Aoubiza, S. Mohammadi, A. Adibi, and V. Laude, Phys. Rev. E **74**, 046610 (2006).
[12] J. O. Vasseur, P. A. Deymier, B. Chenni, B. Djafari-Rouhani, L. Dobrzynski, and D. Prevost, Phys. Rev. Lett. **86**, 3012 (2001).
[13] V. Laude, M. Wilm, S. Benchabane, and A. Khelif, Phys. Rev. E **71**, 036607 (2005).
[14] B. Bonello, C. Charles, and F. Ganot, Appl. Phys. Lett. **90**, 021909 (2007).
[15] J. J. Chen, K. W. Zhang, J. Gao, and J. C. Cheng, Phys. Rev. B **73**, 094307 (2006).
[16] J. H. Sun and T. T. Wu, Phys. Rev. B **76**, 104304 (2007).
[17] Z. L. Hou and B. M. Assouar, Phys. Lett. A **372**, 2091 (2008).
[18] B. Manzanares-Martinez and F. Ramos-Mendieta, Phys. Rev. B **68**, 134303 (2003).
[19] J. O. Vasseur, P. A. Deymier, B. Djafari-Rouhani, and Y. Pennec, Proceedings of IMECE 2006, ASME International Mechanical Engineering Congress and Exposition, Chicago, Illinois, 2006.
[20] J. O. Vasseur, P. A. Deymier, B. Djafari-Rouhani, Y. Pennec, and A. C. Hladky-Hennion, Phys. Rev. B **77**, 085415 (2008).
[21] Q. Ni and J. C. Cheng, Phys. Rev. B **72**, 014305 (2005).
[22] Z. L. Hou, F. G. Wu, X. J. Fu, and Y. Y. Liu, Phys. Rev. E **71**, 037604 (2005).
[23] L. P. Solie and B. A. Auld, J. Acoust. Soc. Am. **54**, 50 (1973).
[24] S. G. Joshi and Y. Jin, J. Appl. Phys. **69**, 8018 (1991).